PERGAMON

International Journal of Solids and Structures 38 (2001) 3759–3770

INTERNATIONAL JOURNAL OF SOLIDS and STRUCTURES

www.elsevier.com/locate/ijsolstr

Compressive fracture of non-linear composites undergoing large deformations

Igor A. Guz, Costas Soutis *

Department of Aeronautics, Imperial College of Science Technology and Medicine, Prince Consort Road, London SW7 2BY, UK

Received 20 October 1999; in revised form 25 May 2000

Abstract

Based on the results obtained within the scope of the model of piecewise-homogeneous medium and three-dimensional stability theory, the accuracy of the continuum theory is examined for laminated incompressible materials undergoing large deformations. Estimation of the accuracy of the continuum theory is illustrated by numerical results for the particular models of composites when the layers are hyperelastic materials with the elastic potential of the neo-Hookean type (Treloar's potential). Based on this the influence of the layers' thickness and their stiffness on the accuracy of the continuum theory is determined. © 2001 Elsevier Science Ltd. All rights reserved.

Keywords: Laminated composite materials; Instability; Compression; Fracture; Continuum; Non-linear; Large deformation; Homogenisation

1. Introduction

One of the most interesting and inadequately investigated phenomena in mechanics of composites is fracture (instability) in compression when mechanisms of failure, specific to heterogeneous media only, are revealed. It should be underlined that zones of compressive stresses can appear in composite structures even under tensile loads. They could be due to the presence of holes, cut-outs and cracks, or generated by impact. The task of deriving three-dimensional (3-D) analytical (closed-form) solutions for such problems is considered as one of great importance. Such solutions, if obtained, give the possibility to analyse the behaviour of a structure on the wide range of material properties and to make certain predictions not worrying about applicability of approximate methods.

In mechanics of heterogeneous (piecewise-homogeneous) media, there are two different methods to describe the behaviour of solids. One of them is based on the model of piecewise-homogeneous medium (Fig. 1a), when each component of material is described by 3-D equations of solid mechanics, provided certain boundary conditions are satisfied at the interfaces. This approach enables one to investigate in the

* Corresponding author. Tel.: +44-020-7594-6070; fax: +44-020-7584-8120.
E-mail address: c.soutis@ic.ac.uk (C. Soutis).

PII: S0020-7683(00)00237-7

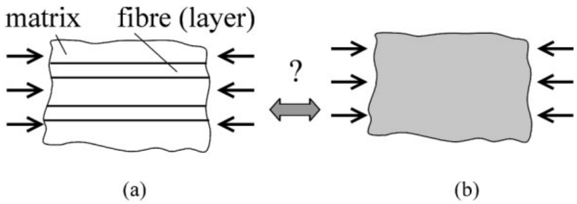

Fig. 1. Model of (a) piecewise-homogeneous medium and (b) continuum theory.

most rigorous way any phenomena in the internal structure of solids. However, due to its complexity this method is restricted to a very small group of problems. The other approach, or continuum theory (Fig. 1b), involves significant simplifications. Within the continuum theory a solid (e.g. a composite) is simulated by homogeneous anisotropic material with effective constants, by means of which physical properties of the original rock, shape and volume fraction of the constituents are taken into account. The continuum theory may be applied when the scale of investigated phenomena (for example, the wavelength of the mode of stability loss l) is considerably larger than the scale of material structure (say, the layer thickness h), i.e.

$$l \gg h. \tag{1}$$

The approach based on the model of piecewise-homogeneous medium is free from such restrictions and is, therefore, the most accurate one.

The wide usage of the continuum theory due to its simplicity in comparison with the model of piecewise-homogeneous medium puts into consideration the questions of its accuracy and of its domain of applicability. The answer to it can be given by comparison of the results delivered by both continuum theory and the most accurate approach; the latter imposes no restrictions on the scale of investigated phenomena, and therefore, has a much larger domain of applicability than the first one. The results obtained within the continuum theory must follow from those obtained using the model of piecewise-homogeneous medium if the ratio between the scale of structure and the scale of phenomenon tends to zero, i.e. when

$$hl^{-1} \to 0. \tag{2}$$

If this is the case, the continuum theory can be regarded as asymptotically accurate.

Except the exact approaches, which are based on the 3-D stability theory expounded, for instance, in the work of Guz (1999), there are also approximate approaches to the considered problem proposed by Rosen (1965) and by many other authors. Detailed reviews of these approximate approaches are given, for example, by Soutis (1991,1996), Schultheisz and Waas (1996) and Guz and Lapusta (1999). However, the approximate approaches proved to be not worth applying. This is discussed in some detail in Section 2.

In the past, investigations of the continuum theory accuracy in relation to the model of piecewise-homogeneous medium were performed only for other physical phenomena (for example, for the problems of wave propagation) by Rytov (1956) and Brekhovskih (1979) or for other models of layers (namely, compressible linear elastic) by Guz and Soutis (1999a,b, 2000). Besides this, validation of the Cosserat-continuum approach to buckling of linear elastic medium was considered by Papamichos et al. (1990) and Vardoulakis and Sulem (1995), where only numerical solutions by the "transfer matrix technique" for particular layered media were used. But, there are not yet such investigations for problems on stability loss in composite structures undergoing finite (large) deformations. This paper attempts to fill that gap. It is devoted to substantiation of the continuum theory (Guz, 1990) applied to predict fracture of a laminated composite material with a periodical structure undergoing large deformations in uniaxial compression. Within the scope of this theory, the moment of stability loss in the structure of the material – internal instability according to Biot (1965) – is treated as the beginning of the fracture process. Special attention is paid to the calculation of the continuum theory accuracy for the particular laminated composites consisting of hyperelastic materials, taking into account the influence of geometrical and mechanical properties of the individual layers.

2. Instability (microbuckling) of composites under large deformations

2.1. Problem statement within the scope of the piecewise-homogeneous medium model

Let us briefly consider the statement of the stability problem (microbuckling) for composites undergoing large deformations. Let the composite consists of alternating layers with thicknesses $2h_r$ and $2h_m$ (Fig. 2), which are simulated by incompressible, non-linear, elastic, isotropic or orthotropic solids with general form of constitutive equations. The material is uniaxially compressed in the plane of layers by "dead" loads applied at infinity in such a manner that equal deformations along all layers are provided and, therefore, the plain strain problem should be considered. Since the analysis is based on previous works by the authors (Guz and Soutis, 1999a,b) and on general approaches developed by Guz (1990, 1999), some equations derived earlier will be given for the sake of clarity.

Within the scope of the most accurate approach, i.e. using the model of piecewise-homogeneous medium and equations of the 3-D linearised stability theory by Guz (1999), we have to solve the following eigenvalue problem. Henceforth all values corresponding to the precritical state will be marked by the superscript '0' to distinguish them from perturbations of the same values. Indices r and m show that the value is relevant to fibre (reinforcement) or matrix, respectively. The axial displacement, u_i^0, and strain, ε_{ij}^0, (in terms of the shortening factor λ_j in the direction of OX_j axis) for the considered type of loading are

$$u_i^0 = (\lambda_i - 1)x_i, \quad \lambda_i = \text{const}, \qquad \varepsilon_{ij}^0 = (\lambda_i - 1)\delta_{ij}, \quad \text{where } \delta_{ij} \text{ is the Kronecker symbol.} \tag{3}$$

The stability equations for the individual layers are

$$\frac{\partial}{\partial x_i} t_{ij}^{\mathrm{r}} = 0, \quad \frac{\partial}{\partial x_i} t_{ij}^{\mathrm{m}} = 0, \qquad i, j = 1, 2, 3. \tag{4}$$

The non-symmetrical stress tensor t_{ij} is referred to the unit area of the relevant surface elements in the undeformed state (in the reference configuration). Namely, t_{ij} is a stress component acting in direction of OX_j at the elementary area with normal OX_i. This is non-symmetrical Piola–Kirchhoff stress tensor or nominal stress tensor using the terminology of Hill (1958). Further, we shall consider also the symmetrical stress tensor S_{ij} which reduces to σ_{ij} for the case of small precritical deformations. For incompressible solids, stresses are related to displacements by (p is hydrostatic pressure)

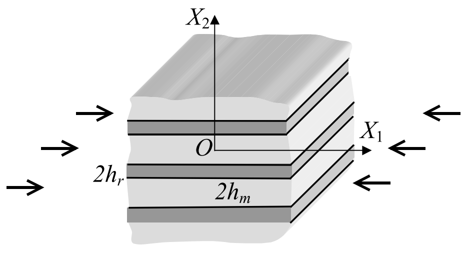

Fig. 2. The co-ordinate system and applied loads (uniform uniaxial compression).

$$t_{ij} = \kappa_{ij\alpha\beta}\frac{\partial u_\alpha}{\partial x_\beta} + \delta_{ij}q_j p, \quad q_i = \lambda_i^{-1} \tag{5}$$

with the incompressibility condition

$$\lambda_1\lambda_2\lambda_3 = 1. \tag{6}$$

Components of the tensor κ depend on material properties and on loads (i.e. on precritical state). The quantity characterising the precritical state, i.e. stress S_{ij}^0 or strain ε_{ij}^0, is the parameter with respect to which the eigenvalue problem should be solved. In the most general case

$$\kappa_{ij\alpha\beta} = \lambda_j\lambda_\alpha[\delta_{ij}\delta_{\alpha\beta}A_{\beta i} + (1-\delta_{ij})(\delta_{i\alpha}\delta_{j\beta}\mu_{ij} + \delta_{i\beta}\delta_{j\alpha}\mu_{ji})] + \delta_{i\beta}\delta_{j\alpha}S_{\beta\beta}^0. \tag{7}$$

The particular expressions for $\kappa_{ij\alpha\beta}$ for numerous kinds of constitutive equations were obtained by Guz (1999). For example, for general elastic solids,

$$A_{\beta i} = A_{\beta i}(f, \lambda_j^0, S_{nl}^0) \quad \text{and} \quad \mu_{\beta i} = \mu_{\beta i}(f, \lambda_j^0, S_{nl}^0), \tag{8}$$

where

$$S_{ij}^0 = f(\varepsilon_{11}^0, \varepsilon_{12}^0, \ldots, \varepsilon_{33}^0). \tag{9}$$

For hyperelastic solids, if Φ is the strain energy density function (elastic potential),

$$A_{\beta i} = A_{\beta i}(\Phi, \varepsilon_{nl}^0) \quad \text{and} \quad \mu_{\beta i} = \mu_{\beta i}(\Phi, \varepsilon_{nl}^0). \tag{10}$$

To complete the problem statement, the boundary conditions should be written for each individual interface, i.e.

$$t_{22}^{\rm r} = t_{22}^{\rm m}, \quad t_{12}^{\rm r} = t_{12}^{\rm m}, \quad u_2^{\rm r} = u_2^{\rm m}, \quad u_1^{\rm r} = u_1^{\rm m}. \tag{11}$$

Characteristic determinants were derived for the plane (Guz, 1982) and for non-axisymmetrical 3-D problems (Guz, 1989) by the most accurate approach (i.e. within the model of piecewise-homogeneous medium) for four modes of stability loss (Fig. 3). For example, for the case of uniaxial compression (Fig. 2) they can be expressed as

$$\det\|\beta_{\rm rs}\| = 0, \quad {\rm r, s} = 1, 2, 3, 4, \tag{12}$$

where for the first mode of stability loss, which is called the shear mode according to Rosen (1965),

$$\begin{aligned}
&\beta_{11} = (\lambda_1^{-2}\kappa_{1212}^{\rm m} + \eta_2^{\rm m^2}\kappa_{2112}^{\rm m})\cosh\alpha_{\rm m}\eta_2^{\rm m}, \quad \beta_{12} = (\lambda_1^{-2}\kappa_{1212}^{\rm m} + \eta_3^{\rm m^2}\kappa_{2112}^{\rm m})\cosh\alpha_{\rm m}\eta_3^{\rm m},\\
&\beta_{13} = (\lambda_1^{-2}\kappa_{1212}^{\rm r} + \eta_2^{\rm r^2}\kappa_{2112}^{\rm r})\cosh\alpha_{\rm r}\eta_2^{\rm r}, \quad \beta_{14} = (\lambda_1^{-2}\kappa_{1212}^{\rm r} + \eta_3^{\rm r^2}\kappa_{2112}^{\rm r})\cosh\alpha_{\rm r}\eta_3^{\rm r},\\
&\beta_{21} = (\lambda_1^2\eta_2^{\rm m^2}\kappa_{2112}^{\rm m} - \lambda_1^{-2}\kappa_{2222}^{\rm m} - \lambda_1^2\kappa_{1111}^{\rm m} + 2\kappa_{1122}^{\rm m} + \kappa_{1212}^{\rm m})\eta_2^{\rm m}\sinh\alpha_{\rm m}\eta_2^{\rm m},\\
&\beta_{22} = (\lambda_1^2\eta_3^{\rm m^2}\kappa_{2112}^{\rm m} - \lambda_1^{-2}\kappa_{2222}^{\rm m} - \lambda_1^2\kappa_{1111}^{\rm m} + 2\kappa_{1122}^{\rm m} + \kappa_{1212}^{\rm m})\eta_3^{\rm m}\sinh\alpha_{\rm m}\eta_3^{\rm m},\\
&\beta_{23} = (\lambda_1^2\eta_2^{\rm r^2}\kappa_{2112}^{\rm r} - \lambda_1^{-2}\kappa_{2222}^{\rm r} - \lambda_1^2\kappa_{1111}^{\rm r} + 2\kappa_{1122}^{\rm r} + \kappa_{1212}^{\rm r})\eta_2^{\rm r}\sinh\alpha_{\rm r}\eta_2^{\rm r},\\
&\beta_{24} = (\lambda_1^2\eta_3^{\rm r^2}\kappa_{2112}^{\rm r} - \lambda_1^{-2}\kappa_{2222}^{\rm r} - \lambda_1^2\kappa_{1111}^{\rm r} + 2\kappa_{1122}^{\rm r} + \kappa_{1212}^{\rm r})\eta_3^{\rm r}\sinh\alpha_{\rm r}\eta_3^{\rm r},\\
&\beta_{31} = \eta_2^{\rm m}\sinh\alpha_{\rm m}\eta_2^{\rm m}, \quad \beta_{32} = \eta_3^{\rm m}\sinh\alpha_{\rm m}\eta_3^{\rm m}, \quad \beta_{33} = \eta_2^{\rm r}\sinh\alpha_{\rm r}\eta_2^{\rm r}, \quad \beta_{34} = \eta_3^{\rm r}\sinh\alpha_{\rm r}\eta_3^{\rm r},\\
&\beta_{41} = \lambda_1^{-2}\cosh\alpha_{\rm m}\eta_2^{\rm m}, \quad \beta_{42} = \lambda_1^{-2}\cosh\alpha_{\rm m}\eta_3^{\rm m}, \quad \beta_{43} = \lambda_1^{-2}\cosh\alpha_{\rm r}\eta_2^{\rm r}, \quad \beta_{44} = \lambda_1^{-2}\cosh\alpha_{\rm r}\eta_3^{\rm r}
\end{aligned} \tag{13}$$

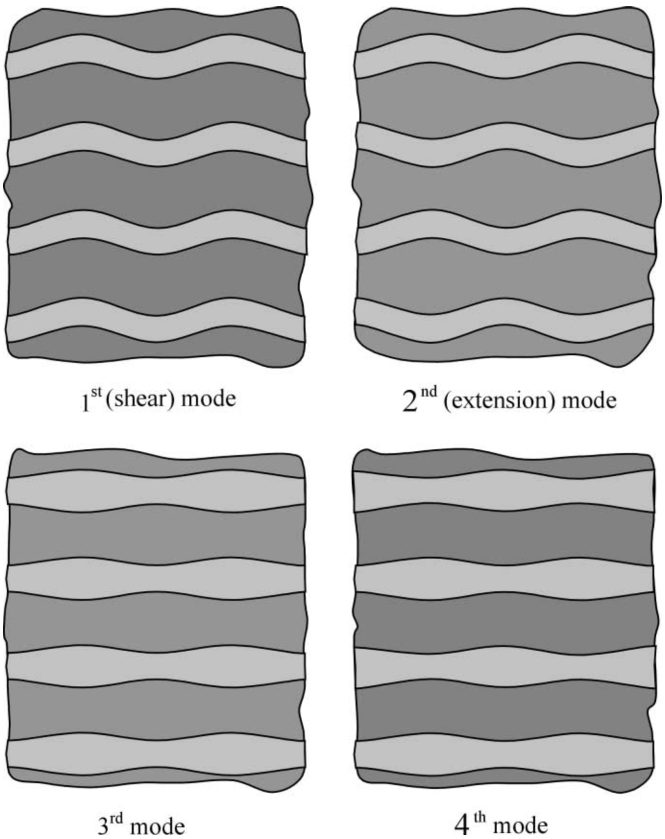

Fig. 3. Modes of stability loss.

and for the second mode of stability loss, which is called the extension mode according to Rosen (1965),

$$
\begin{aligned}
&\beta_{11} = (\lambda_1^{-2}\kappa^{\mathrm{m}}_{1212} + \eta_2^{\mathrm{m}^2}\kappa^{\mathrm{m}}_{2112})\sinh\alpha_{\mathrm{m}}\eta_2^{\mathrm{m}}, \quad \beta_{12} = (\lambda_1^{-2}\kappa^{\mathrm{m}}_{1212} + \eta_3^{\mathrm{m}^2}\kappa^{\mathrm{m}}_{2112})\sinh\alpha_{\mathrm{m}}\eta_3^{\mathrm{m}},\\
&\beta_{13} = (\lambda_1^{-2}\kappa^{\mathrm{r}}_{1212} + \eta_2^{\mathrm{r}^2}\kappa^{\mathrm{r}}_{2112})\sinh\alpha_{\mathrm{r}}\eta_2^{\mathrm{r}}, \quad \beta_{14} = (\lambda_1^{-2}\kappa^{\mathrm{r}}_{1212} + \eta_3^{\mathrm{r}^2}\kappa^{\mathrm{r}}_{2112})\sinh\alpha_{\mathrm{r}}\eta_3^{\mathrm{r}},\\
&\beta_{21} = (\lambda_1^2\eta_2^{\mathrm{m}^2}\kappa^{\mathrm{m}}_{2112} - \lambda_1^{-2}\kappa^{\mathrm{m}}_{2222} - \lambda_1^2\kappa^{\mathrm{m}}_{1111} + 2\kappa^{\mathrm{m}}_{1122} + \kappa^{\mathrm{m}}_{1212})\eta_2^{\mathrm{m}}\cosh\alpha_{\mathrm{m}}\eta_2^{\mathrm{m}},\\
&\beta_{22} = (\lambda_1^2\eta_3^{\mathrm{m}^2}\kappa^{\mathrm{m}}_{2112} - \lambda_1^{-2}\kappa^{\mathrm{m}}_{2222} - \lambda_1^2\kappa^{\mathrm{m}}_{1111} + 2\kappa^{\mathrm{m}}_{1122} + \kappa^{\mathrm{m}}_{1212})\eta_3^{\mathrm{m}}\cosh\alpha_{\mathrm{m}}\eta_3^{\mathrm{m}},\\
&\beta_{23} = (\lambda_1^2\eta_2^{\mathrm{r}^2}\kappa^{\mathrm{r}}_{2112} - \lambda_1^{-2}\kappa^{\mathrm{r}}_{2222} - \lambda_1^2\kappa^{\mathrm{r}}_{1111} + 2\kappa^{\mathrm{r}}_{1122} + \kappa^{\mathrm{r}}_{1212})\eta_2^{\mathrm{r}}\cosh\alpha_{\mathrm{r}}\eta_2^{\mathrm{r}},\\
&\beta_{24} = (\lambda_1^2\eta_3^{\mathrm{r}^2}\kappa^{\mathrm{r}}_{2112} - \lambda_1^{-2}\kappa^{\mathrm{r}}_{2222} - \lambda_1^2\kappa^{\mathrm{r}}_{1111} + 2\kappa^{\mathrm{r}}_{1122} + \kappa^{\mathrm{r}}_{1212})\eta_3^{\mathrm{r}}\cosh\alpha_{\mathrm{r}}\eta_3^{\mathrm{r}},\\
&\beta_{31} = \eta_2^{\mathrm{m}}\cosh\alpha_{\mathrm{m}}\eta_2^{\mathrm{m}}, \quad \beta_{32} = \eta_3^{\mathrm{m}}\cosh\alpha_{\mathrm{m}}\eta_3^{\mathrm{m}}, \quad \beta_{33} = \eta_2^{\mathrm{r}}\cosh\alpha_{\mathrm{r}}\eta_2^{\mathrm{r}}, \quad \beta_{34} = \eta_3^{\mathrm{r}}\cosh\alpha_{\mathrm{r}}\eta_3^{\mathrm{r}},\\
&\beta_{41} = \lambda_1^{-2}\sinh\alpha_{\mathrm{m}}\eta_2^{\mathrm{m}}, \quad \beta_{42} = \lambda_1^{-2}\sinh\alpha_{\mathrm{m}}\eta_3^{\mathrm{m}}, \quad \beta_{43} = \lambda_1^{-2}\sinh\alpha_{\mathrm{r}}\eta_2^{\mathrm{r}}, \quad \beta_{44} = \lambda_1^{-2}\sinh\alpha_{\mathrm{r}}\eta_3^{\mathrm{r}}.
\end{aligned}
\tag{14}
$$

Normalised wavelengths α_{r} and α_{m} are related to the layer thickness and to the half-wavelength, *l,* of modes of stability loss along the OX_1 axis as

$$
\alpha_{\mathrm{r}} = \pi h_{\mathrm{r}} l^{-1}, \quad \alpha_{\mathrm{m}} = \pi h_{\mathrm{m}} l^{-1}. \tag{15}
$$

2.2. On the applicability of the approximate approach

The approximate theories do not describe the phenomenon under consideration even on the qualitative level. It was proved (Guz, 1990; Guz and Soutis, 1999b) that they give a huge discrepancy in comparison with the exact approach and with experimental data. For example, even for the simplest case of all linear elastic compressible layers of a composite undergoing small precritical deformations and considered within the scope of geometrically linear theory, the Rosen model (Rosen, 1965) for the shear and extension modes are not worth applying. Indeed, the Rosen model may give not only critical strains which are significantly higher than those obtained by the exact approach but sometimes predicts even the mode of stability loss different from that obtained within the exact approach. Moreover, even the continuum theory (Guz, 1990) based on equations of the 3-D stability theory (i.e. the exact approach) gives much better results than the Rosen model. Indeed, critical strains predicted by the Rosen model for the shear mode are always higher than those measured by Soutis (1991) or predicted by the continuum theory, and for small volume fractions of matrix the approximate approach gives just physically unrealistic strength limits. In spite of using the model of piecewise-homogeneous medium, the Rosen theory involves considerable simplifications: modelling of the stiff layers by the thin beam theory and the one-dimensional model for the matrix. It makes the results of this method inaccurate even for simple cases. For more complicated models which take into account large deformations and geometrical and physical non-linearity (e.g. those considered in this paper), the approximate theory is definitely inapplicable and one can expect even a bigger difference between the exact and approximate approaches.

3. Analysis of solutions obtained by the model of piecewise-homogeneous medium

3.1. Limit transition to the long-wave asymptotic

To perform the asymptotic analysis we should apply the condition of applicability of the continuum theory (Eq. (2)) to all formulae and calculate the limits analytically under this condition, which yields

$$\begin{aligned} &\alpha_{\mathrm{r}} \to 0, \quad \alpha_{\mathrm{m}} \to 0, \quad \cosh \alpha_{\mathrm{r}} \eta_j^{\mathrm{r}} \to 1, \quad \cosh \alpha_{\mathrm{m}} \eta_j^{\mathrm{m}} \to 1, \quad \sinh \alpha_{\mathrm{r}} \eta_j^{\mathrm{r}} \to \alpha_{\mathrm{r}} \eta_j^{\mathrm{r}}, \\ &\sinh \alpha_{\mathrm{m}} \eta_j^{\mathrm{m}} \to \alpha_{\mathrm{m}} \eta_j^{\mathrm{m}}, \qquad j = 2, 3. \end{aligned} \tag{16}$$

As a result of such manipulations, we can obtain the long-wave approximation (if $\alpha \to 0$ then $l \to \infty$). On substitution of Eq. (16) into characteristic determinants (12) derived earlier, we find, after a number of rearrangements, that the characteristic equations reduce to the following:

- For the first mode of stability loss

$$\frac{(\eta_2^{\mathrm{r}^2} - \eta_3^{\mathrm{r}^2})(\eta_2^{\mathrm{m}^2} - \eta_3^{\mathrm{m}^2})\pi^2}{l^2 \lambda_1^2} \left[\frac{h_{\mathrm{m}}}{h_{\mathrm{r}}} (\kappa_{1212}^{\mathrm{m}} - \kappa_{1212}^{\mathrm{r}})^2 - \left(\frac{h_{\mathrm{m}}}{h_{\mathrm{r}}} \kappa_{1221}^{\mathrm{m}} + \kappa_{1221}^{\mathrm{r}} \right) \left(\kappa_{2112}^{\mathrm{m}} + \frac{h_{\mathrm{m}}}{h_{\mathrm{r}}} \kappa_{2112}^{\mathrm{r}} \right) \right] = 0. \tag{17}$$

- Second mode of stability loss

$$(\eta_2^{\mathrm{r}^2} - \eta_3^{\mathrm{r}^2})(\eta_2^{\mathrm{m}^2} - \eta_3^{\mathrm{m}^2})\eta_2^{\mathrm{m}} \eta_3^{\mathrm{m}} \lambda_1^2 \kappa_{2112}^{\mathrm{m}} \kappa_{2112}^{\mathrm{r}} = 0. \tag{18}$$

- Third mode of stability loss

$$(\eta_2^{\mathrm{r}^2} - \eta_3^{\mathrm{r}^2})(\eta_2^{\mathrm{m}^2} - \eta_3^{\mathrm{m}^2})\eta_2^{\mathrm{r}} \eta_3^{\mathrm{r}} \eta_2^{\mathrm{m}} \eta_3^{\mathrm{m}} \frac{\pi^2}{l^2} \lambda_1^2 \kappa_{2112}^{\mathrm{m}} \kappa_{2112}^{\mathrm{r}} \left(\frac{h_{\mathrm{m}}}{h_{\mathrm{r}}} + 1 \right) = 0. \tag{19}$$

- Fourth mode of stability loss

$$(\eta_2^{\mathrm{r}^2} - \eta_3^{\mathrm{r}^2})(\eta_2^{\mathrm{m}^2} - \eta_3^{\mathrm{m}^2})\eta_2^{\mathrm{r}} \eta_3^{\mathrm{r}} \lambda_1^2 \kappa_{2112}^{\mathrm{m}} \kappa_{2112}^{\mathrm{r}} = 0. \tag{20}$$

3.2. Analysis of equations for the particular modes of instability

Let us examine the characteristic Eqs. (17)–(20), which correspond, after the limit transition, to the continuum theory. It was proved that for the considered models of layers, the roots of the characteristic equations (i.e. parameters $(\eta_j^{\mathrm{r}})^2$and$(\eta_j^{\mathrm{m}})^2$, which depend on the components of tensor κ and therefore on properties of the layers and applied loads) are always real and positive. This means, that

$$\begin{aligned} &\mathrm{Re}(\eta_2^{\mathrm{r}})^2 > 0, \quad \mathrm{Im}(\eta_2^{\mathrm{r}})^2 = 0, \quad \mathrm{Re}(\eta_2^{\mathrm{m}})^2 > 0, \quad \mathrm{Im}(\eta_2^{\mathrm{m}})^2 = 0, \\ &\mathrm{Re}(\eta_3^{\mathrm{r}})^2 > 0, \quad \mathrm{Im}(\eta_3^{\mathrm{r}})^2 = 0, \quad \mathrm{Re}(\eta_3^{\mathrm{m}})^2 > 0, \quad \mathrm{Im}(\eta_3^{\mathrm{m}})^2 = 0. \end{aligned} \tag{21}$$

Also, it is obvious that the solutions, which correspond to the considered phenomenon of internal instability, must depend on the properties of both alternating layers, i.e. on the ratio h_r/h_{m}.

Taking into account Eq. (21), one can check that Eqs. (18)–(20), which correspond to the second, third and fourth modes of stability loss, respectively, do not have such solutions and, therefore, do not describe the internal instability in the long-wave approximation. It also means that modes of stability loss, other than the first (shear) mode, cannot be described by the continuum theory. Of course, the equations for these modes might have roots within the most accurate approach, i.e. within the model of piecewise-homogeneous medium, Eq. (12). The example of the second mode having roots will be given later in Fig. 4.

Eq. (8), which corresponds to the first mode of stability loss, generally speaking, may have roots related to the internal instability of the considered materials. This needs a more detailed investigation, which is the next task. For the further analysis, components of tensor κ can be expressed (Guz, 1999) as

$$\begin{aligned} &\kappa_{2112}^{\mathrm{r}} = \lambda_1^2 \mu_{12}^{\mathrm{r}}, \quad \kappa_{1221}^{\mathrm{r}} = \lambda_1^{-2} \mu_{12}^{\mathrm{r}} + (S_{11}^0)^{\mathrm{r}}, \quad \kappa_{1212}^{\mathrm{r}} = \mu_{12}^{\mathrm{r}}, \\ &\kappa_{2112}^{\mathrm{m}} = \lambda_1^2 \mu_{12}^{\mathrm{m}}, \quad \kappa_{1221}^{\mathrm{m}} = \lambda_1^{-2} \mu_{12}^{\mathrm{m}} + (S_{11}^0)^{\mathrm{m}}, \quad \kappa_{1212}^{\mathrm{m}} = \mu_{12}^{\mathrm{m}}. \end{aligned} \tag{22}$$

Substituting Eq. (22) into characteristic Eq. (17), for the first (shear) mode we derive

$$\frac{h_{\mathrm{m}}}{h_{\mathrm{r}}}(\mu_{12}^{\mathrm{r}} - \mu_{12}^{\mathrm{m}})^2 - \left[\mu_{12}^{\mathrm{r}} + \frac{h_{\mathrm{m}}}{h_{\mathrm{r}}}\mu_{12}^{\mathrm{m}} + \lambda_1^2\left((S_{11}^0)^{\mathrm{r}} + \frac{h_{\mathrm{m}}}{h_{\mathrm{r}}}(S_{11}^0)^{\mathrm{m}}\right)\right]\left(\mu_{12}^{\mathrm{m}} + \frac{h_{\mathrm{m}}}{h_{\mathrm{r}}}\mu_{12}^{\mathrm{r}}\right) = 0. \tag{23}$$

In order to analyse Eq. (23), the effective values of stresses and of quantity μ_{12}, denoted respectively as $\langle S_{11}^0 \rangle$ and $\langle \mu_{12} \rangle$, will be utilised. At the moment of material stability loss they can be calculated as

$$\langle S_{11}^0 \rangle = (S_{11}^0)^{\mathrm{r}} V_{\mathrm{r}}^* + (S_{11}^0)^{\mathrm{m}} V_{\mathrm{m}}^*, \qquad \langle \mu_{12} \rangle = \mu_{12}^{\mathrm{r}} \mu_{12}^{\mathrm{m}} (\mu_{12}^{\mathrm{r}} V_{\mathrm{m}}^* + \mu_{12}^{\mathrm{m}} V_{\mathrm{r}}^*)^{-1}, \tag{24}$$

where V_{r}^* and V_{m}^* are the volume fractions of the components in the deformed state. Due to the kind of applied loads (Fig. 2), the volume fractions of the components in the undeformed ($V_{\mathrm{r}}, V_{\mathrm{m}}$) and deformed states are equal for the same components. Indeed, taking account of Eq. (3) we have

$$V_{\mathrm{r}}^* = \frac{\lambda_2^{\mathrm{r}} h_{\mathrm{r}}}{\lambda_2^{\mathrm{r}} h_{\mathrm{r}} + \lambda_2^{\mathrm{m}} h_{\mathrm{m}}} = \frac{h_{\mathrm{r}}}{h_{\mathrm{r}} + h_{\mathrm{m}}} = V_{\mathrm{r}}, \quad V_{\mathrm{m}}^* = \frac{\lambda_2^{\mathrm{m}} h_{\mathrm{m}}}{\lambda_2^{\mathrm{r}} h_{\mathrm{r}} + \lambda_2^{\mathrm{m}} h_{\mathrm{m}}} = \frac{h_{\mathrm{m}}}{h_{\mathrm{r}} + h_{\mathrm{m}}} = V_{\mathrm{m}}. \tag{25}$$

Let us denote the theoretical strength limit as $(\Pi_1^-)_{\mathrm{T}}$. Substituting Eqs. (15) and (16) into Eq. (14), after some rearrangement, we get

$$(\Pi_1^-)_{\mathrm{T}} \equiv -\langle S_{11}^0 \rangle = \lambda_1^{-2} \langle \mu_{12} \rangle. \tag{26}$$

This coincides with the results derived within the scope of the continuum theory (Guz, 1990) as applied to non-linear laminated composites undergoing large deformations. Typical critical values of λ_1 are presented in Section 4 for neo-Hookean materials.

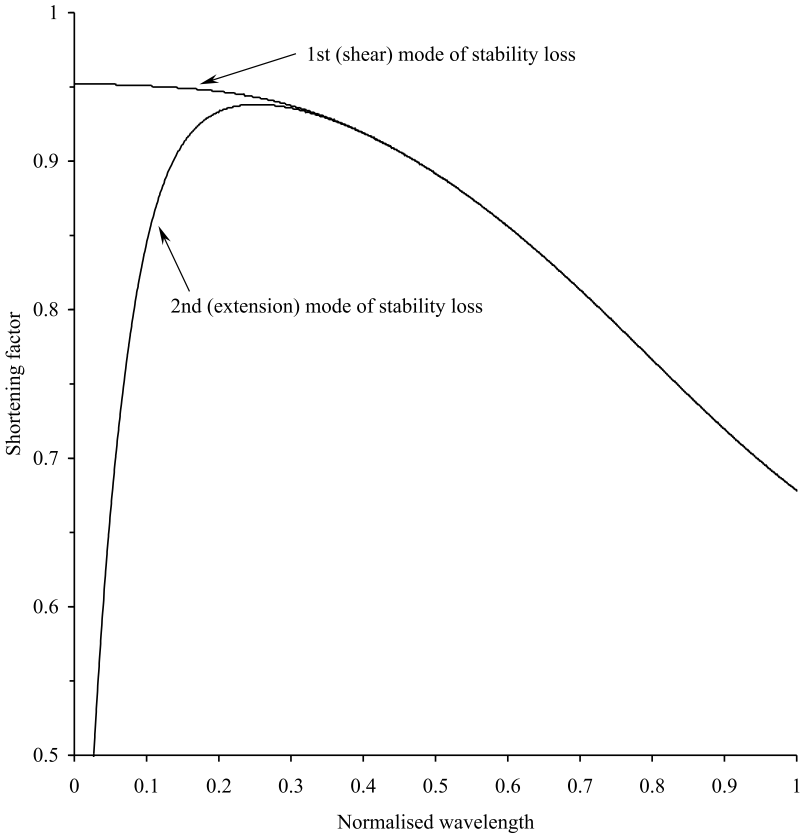

Fig. 4. Solutions of the characteristic equations for the case of the most accurate problem statement: values of λ_1 (shortening factor) plotted against α_r (normalised wavelength) for the first (shear) and second (extension) modes of stability loss; $C^r_{10}/C^m_{10} = 50$, $h_r/h_m = 0.12$.

It should be noted that within the scope of the continuum theory, Eq. (26) gives the theoretical strength limit for non-linear, elastic, incompressible composites as a function of $\langle\mu_{12}\rangle$, i.e. the effective value of quantity μ_{12}, which is related to the material properties by Eq. (24). This theoretical strength limit is written for the general form of constitutive equations for layers. If one needs a concrete expression for particular kind of the layers' properties, it can be determined using the formulae for μ^r_{12} and μ^m_{12} presented by Guz (1990, 1999). For example, for the case of all linear elastic, isotropic, compressible layers

$$(\Pi_1^-)_T \equiv -\langle\sigma^0_{11}\rangle = \langle G_{12}\rangle, \tag{27}$$

where $\langle G_{12}\rangle$ is the effective shear modulus of the laminated composite.

Thus, it is rigorously proved for laminated, non-linear, elastic composites undergoing large deformations in uniaxial compression that the results of the continuum theory follow as a long-wave approximation from those for the first mode of stability loss obtained using the model of piecewise-homogeneous medium. Therefore, the asymptotic accuracy of the continuum theory for such composites is established.

It should be underlined that the analytical 3-D approach developed in the present subsection can be applied not only to laminated composites but to any piecewise-homogeneous, layered system with similar constituent properties undergoing uniaxial compression.

4. Results for hyperelastic non-linear materials

4.1. Treloar's potential

As an example, let us consider a composite consisting of alternating, non-linear, elastic, isotropic, incompressible layers with different properties (Fig. 2). Suppose also that materials of these layers are hyperelastic (Eq. 10), and the simplified version of Mooney's potential, namely neo-Hookean potential, may be chosen for their description in the following form:

$$\Phi^{\mathrm{r}} = 2C_{10}^{\mathrm{r}} I_1^{\mathrm{r}}(\varepsilon_{ij}^0), \quad \Phi^{\mathrm{m}} = 2C_{10}^{\mathrm{m}} I_1^{\mathrm{m}}(\varepsilon_{ij}^0), \tag{28}$$

where C_{10} is a material constant and $I_1(\varepsilon)$ is the first algebraic invariant of Cauchy–Green strain tensor. This potential is also called Treloar's potential, after the author who obtained it from an analysis of model of rubber regarded as a system of long molecular interlinking chains (Treloar, 1955).

It should be noted here that the simpler case (namely, compressible, linear, elastic materials under small deformations) was considered by Guz and Soutis (2000). For transition to the classical linear theory of elasticity under small deformations, we can put in Eq. (28)

$$2C_{10} = G, \quad G = \frac{E}{3}, \qquad v = 0.5. \tag{29}$$

Due to the type of applied loads

$$\lambda_1^{\mathrm{r}} = \lambda_1^{\mathrm{m}} \equiv \lambda_1. \tag{30}$$

Since the plane strain state is considered in the precritical state, from the condition of incompressibility (Eq. (6)) we derive

$$\lambda_3^{\mathrm{r}} = \lambda_3^{\mathrm{m}} = 1, \quad \lambda_2^{\mathrm{r}} = \lambda_2^{\mathrm{m}} = \lambda_1^{-1}. \tag{31}$$

Then for uniaxial compression the components of the tensor κ for this model are expressed, according to Eqs. (3), (5)–(7), (10), (28), (30) and (31), as

$$\begin{aligned}
&\kappa_{1111}^{\mathrm{r}} = 2C_{10}^{\mathrm{r}}(1+\lambda_1^{-4}), \quad \kappa_{2222}^{\mathrm{r}} = 4C_{10}^{\mathrm{r}}, \quad \kappa_{1212}^{\mathrm{r}} = 2C_{10}^{\mathrm{r}}\lambda_1^{-2}, \quad \kappa_{1221}^{\mathrm{r}} = \kappa_{2112}^{\mathrm{r}} = 2C_{10}^{\mathrm{r}}, \quad \kappa_{1122}^{\mathrm{r}} = 0,\\
&\kappa_{1111}^{\mathrm{m}} = 2C_{10}^{\mathrm{m}}(1+\lambda_1^{-4}), \quad \kappa_{2222}^{\mathrm{m}} = 4C_{10}^{\mathrm{m}}, \quad \kappa_{1212}^{\mathrm{m}} = 2C_{10}^{\mathrm{m}}\lambda_1^{-2}, \quad \kappa_{1221}^{\mathrm{m}} = \kappa_{2112}^{\mathrm{m}} = 2C_{10}^{\mathrm{m}}, \quad \kappa_{1122}^{\mathrm{m}} = 0
\end{aligned} \tag{32}$$

and, therefore,

$$\eta_2^{\mathrm{r}} = \lambda_1^{-2}, \quad \eta_3^{\mathrm{r}} = 1, \quad \eta_2^{\mathrm{m}} = \lambda_1^{-2}, \quad \eta_3^{\mathrm{m}} = 1. \tag{33}$$

Substituting Eqs. (32) and (33) into the characteristic equations (12) derived earlier for the four considered modes of stability loss, four transcendental equations were deduced for the case of the model of piecewise-homogeneous medium. Then for each of the modes we have a different characteristic equation in terms of two variables, λ_1 (shortening factor) and α_{r} (normalised wavelength). For example, after some manipulations (Guz, 1982), the equations become

- for the first (shear) mode, from Eqs. (12), (13), (32) and (33),

$$\begin{aligned}
&-\lambda_1^{-2}(1+\lambda_1^4)^2[1 - C_{10}^{\mathrm{r}}(C_{10}^{\mathrm{m}})^{-1}]^2 \tanh\alpha_{\mathrm{r}}\lambda_1^{-2} \tanh\alpha_{\mathrm{m}}\lambda_1^{-2} - 4\lambda_1^2[1 - C_{10}^{\mathrm{r}}(C_{10}^{\mathrm{m}})^{-1}]^2 \tanh\alpha_{\mathrm{r}} \tanh\alpha_{\mathrm{m}}\\
&\quad + [2 - (1+\lambda_1^4)C_{10}^{\mathrm{r}}(C_{10}^{\mathrm{m}})^{-1}]^2 \tanh\alpha_{\mathrm{r}}\lambda_1^{-2} \tanh\alpha_{\mathrm{m}} + [1 + \lambda_1^4 - 2C_{10}^{\mathrm{r}}(C_{10}^{\mathrm{m}})^{-1}]^2 \tanh\alpha_{\mathrm{r}} \tanh\alpha_{\mathrm{m}}\lambda_1^{-2}\\
&\quad + (1-\lambda_1^4)^2 C_{10}^{\mathrm{r}}(C_{10}^{\mathrm{m}})^{-1}(\tanh\alpha_{\mathrm{r}} \tanh\alpha_{\mathrm{r}}\lambda_1^{-2} + \tanh\alpha_{\mathrm{m}} \tanh\alpha_{\mathrm{m}}\lambda_1^{-2}) = 0;
\end{aligned} \tag{34}$$

- for the second (extension) mode, from Eqs. (12), (14), (32) and (33),

$$\begin{aligned}&-\lambda_1^{-2}(1+\lambda_1^4)^2[1-C_{10}^{\mathrm{r}}(C_{10}^{\mathrm{m}})^{-1}]^2\tanh\alpha_{\mathrm{r}}\lambda_1^{-2}\coth\alpha_{\mathrm{m}}\lambda_1^{-2}-4\lambda_1^2[1-C_{10}^{\mathrm{r}}(C_{10}^{\mathrm{m}})^{-1}]^2\tanh\alpha_{\mathrm{r}}\coth\alpha_{\mathrm{m}}\\&+[2-(1+\lambda_1^4)C_{10}^{\mathrm{r}}(C_{10}^{\mathrm{m}})^{-1}]^2\tanh\alpha_{\mathrm{r}}\lambda_1^{-2}\coth\alpha_{\mathrm{m}}+[1+\lambda_1^4-2C_{10}^{\mathrm{r}}(C_{10}^{\mathrm{m}})^{-1}]^2\tanh\alpha_{\mathrm{r}}\coth\alpha_{\mathrm{m}}\lambda_1^{-2}\\&+(1-\lambda_1^4)^2C_{10}^{\mathrm{r}}(C_{10}^{\mathrm{m}})^{-1}(\tanh\alpha_{\mathrm{r}}\tanh\alpha_{\mathrm{r}}\lambda_1^{-2}+\coth\alpha_{\mathrm{m}}\coth\alpha_{\mathrm{m}}\lambda_1^{-2})=0.\end{aligned} \tag{35}$$

The shortening factor λ_1 is related to the value of strain ε_{11}^0 by Eq. (1) and is used here for convenience sake. As the result of solution, four dependences $\lambda_1^{(N)}(\alpha_{\mathrm{r}})$ are obtained, where $N = 1, 2, 3, 4$ is the number of mode. The examples of such dependences are presented in Fig. 4 for the first and second modes. The critical value for the particular mode $\lambda_{\mathrm{cr}}^{(N)}$ can be found as a maximum of the corresponding dependence. The maximum of these four values will be the critical shortening factor of internal instability for the considered laminated material determined by the most accurate approach (λ_{cr}).

On the other hand, substitution of Eqs. (32) and (33) into Eqs. (17)–(20) yields the long-wave approximation (i.e. the asymptotic under the condition $\alpha_{\mathrm{r}} \to 0$) for the characteristic equations for this particular model. As was proved in the previous section, the solution of Eq. (17) will correspond to the results of the continuum theory. Hence, the dependence $\lambda_1^{(1)}(\alpha_{\mathrm{r}})$, calculated for the first mode, gives results of the continuum theory $\lambda_{\mathrm{c.t.}}$ if we put $\alpha_{\mathrm{r}} \to 0$. Therefore, the accuracy of the continuum theory Λ (i.e. the

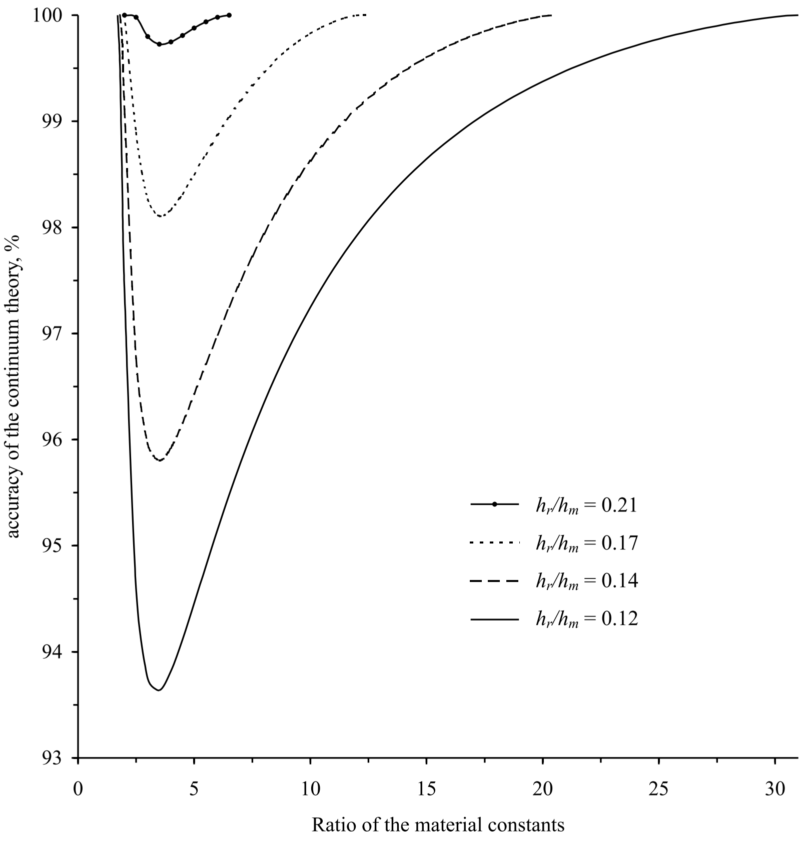

Fig. 5. Values of parameter Λ plotted against $C_{10}^{\mathrm{r}}/C_{10}^{\mathrm{m}}$ for different values of layer thickness ratio $h_{\mathrm{r}}/h_{\mathrm{m}}$.

ratio of the results obtained in the context of the most accurate approach and continuum theory expressed in percentage) will be

$$\Lambda = \frac{\lambda_{\text{c.t.}}}{\lambda_{\text{cr}}} \times 100\% = \frac{\lim\limits_{\alpha_r \to 0} \lambda_1^{(1)}(\alpha_r)}{\max\limits_N \lambda_{\text{cr}}^{(N)}} \times 100\% = \frac{\lim\limits_{\alpha_r \to 0} \lambda_1^{(1)}(\alpha_r)}{\max\limits_N \left(\max\limits_{\alpha_r} \lambda_1^{(N)} \right)} \times 100\%. \tag{36}$$

4.2. Numerical results

Values of the parameter Λ are given in Fig. 5 (for the interval of $1 < \Lambda < 30$) and in Fig. 6 (for the interval of $1 < \Lambda < 100$) in the form of dependences on the ratio of the material constants $C_{10}^{\text{r}}/C_{10}^{\text{m}}$. All eight curves correspond to different values of layer thickness ratio, $h_{\text{r}}/h_{\text{m}}$. It should be noted that for plotting each point on the curves, plots similar to those in Fig. 4 had to be calculated and analysed following Section 4.1. These dependences have strongly non-linear character, proving the importance of taking into account the materials' non-linearity. Another interesting revelation consists of the fact that the minimum values of all curves lie in the very narrow interval of the ratio of the material constants – approximately between $C_{10}^{\text{r}}/C_{10}^{\text{m}} = 3$ and $C_{10}^{\text{r}}/C_{10}^{\text{m}} = 4$. One can also see that larger the ratio $h_{\text{r}}/h_{\text{m}}$, the

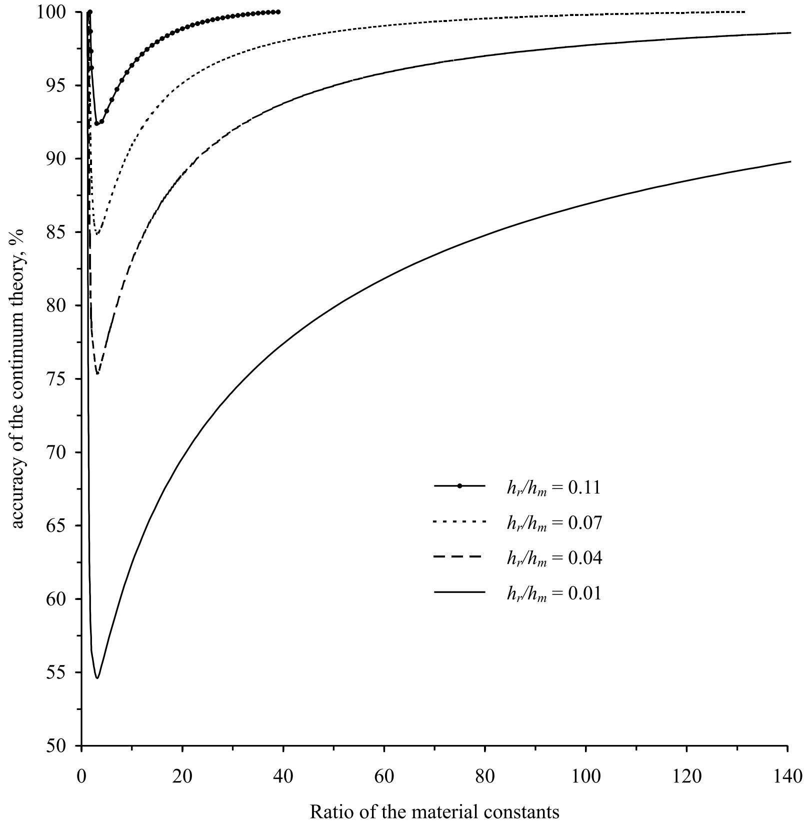

Fig. 6. Values of parameter Λ plotted against $C_{10}^{\text{r}}/C_{10}^{\text{m}}$ for different values of layer thickness ratio $h_{\text{r}}/h_{\text{m}}$.

higher is the accuracy of the continuum theory. It means that the increasing volume fraction of the stiffer layers has a strong impact on the application of the continuum theory in making it more accurate.

5. Conclusions

The asymptotic accuracy of the continuum theory of compressive fracture is established for composites consisting of incompressible, non-linear, elastic, orthotropic layers. It was rigorously proved that the results of the continuum theory follow as a long-wave approximation from those for the first (shear) mode of stability loss obtained using the model of piecewise-homogeneous medium. It is also shown that modes of stability loss, other than the first (shear) mode, cannot be described by the continuum theory. Estimation of accuracy of the continuum theory was obtained by comparison with the critical values, calculated using the model of the piecewise-homogeneous medium (i.e. the most accurate result). This estimation was illustrated in this paper by numerical results for the particular models of hyperelastic layers. At that, the influence of the properties of layers and their thickness ratio on the accuracy of continuum theory was established.

Following the general approach described in this paper the accuracy of the continuum theory as applied to composites with other properties of layers or other kinds of loads can also be investigated.

References

Biot, M.A., 1965. Mechanics of Incremental Deformations. Wiley, New York.

Brekhovskih, L.M., 1979. Waves in Laminated Media. Nauka, Moscow (In Russian).

Guz, A.N., (Ed.), 1982. Mechanics of Composite Materials and Constructive Elements, vol. 1. Naukova Dumka, Kiev (In Russian).

Guz, A.N., 1990. Mechanics of Fracture of Composite Materials in Compression. Naukova Dumka, Kiev (In Russian).

Guz, A.N., 1999. Fundamentals of the Three-Dimensional Theory of Stability of Deformable Bodies. Springer, Berlin.

Guz, A.N., Lapusta, Yu.N., 1999. Three-dimensional problems of the near-surface instability of fiber composites in compression (model of a piecewise-uniform medium). (Survey). International Applied Mechanics 35, 641–670.

Guz, I.A., 1989. Spatial nonaxisymmetric problems of the theory of stability of laminar highly elastic composite materials. Soviet Applied Mechanics 25, 1080–1085.

Guz, I.A., Soutis, C., 1999a. Continuum fracture theory for layered materials: investigation of accuracy. Zeitschrift für Angewandte Mathematik und Mechanik 79, S503–S504.

Guz, I.A., Soutis, C., 1999b. On asymptotic accuracy in continuum fracture mechanics of polymer matrix composites in compression. In: Proceedings of the Fifth International Conference on Deformation and Fracture of Composites, London, UK, March 18–19, 1999. IOM Communications, pp. 211–220.

Guz, I.A., Soutis, C., 2000. A 3-D stability theory applied to layered rocks undergoing finite deformations in biaxial compression. European Journal of Mechanics A/Solids, submitted for publication.

Hill, R., 1958. A general theory of uniqueness and stability of elastic-plastic solids. Journal of Mechanics and Physics of Solids 6, 236–249.

Papamichos, E., Vardoulakis, I., Muhlhaus, H.-B., 1990. Buckling of layered elastic media: a Cosserat-continuum approach and its validation. International Journal of Numerical and Analytical Methods in Geomechanics 14, 473–498.

Rosen, B.W., 1965. Mechanics of Composite Strengthening. In: Fiber Composite Materials. American Society of Metals, Metals Park, pp. 37–75 (Chapter 3).

Rytov, S.M., 1956. Acoustic properties of small-scale-laminated medium. Acoustic Journal 2, 71–83 (In Russian).

Schultheisz, C., Waas, A., 1996. Compressive failure of composites, Parts I and II. Progress in Aerospace Science 32, 1–78.

Soutis, C., 1991. Measurement of the static compressive strength of carbon fibre/epoxy laminates. Composite Science and Technology 42, 373–392.

Soutis, C., 1996. Failure of notched CFRP laminates due to fibre microbuckling: a topical review. Journal of the Mechanical Behaviour of Materials 6, 309–330.

Treloar, L.R.G., 1955. Large elastic deformations in rubber-like materials. In: Proceedings of IUTAM Colloquium. Madrid, Spain, 208–217.

Vardoulakis, I., Sulem, J., 1995. Bifurcation Analysis in Geomechanics. Blackie Academic and Professional, Glasgow.